Implantable device for assisting dementia patients through the stimulation of the olfactory bulb

Alain Aziz
Shiu-Cheng Wang
Adrien Feillard

Contents

1 Summary

Dementia is an increasingly prevalent disease, especially with older adults, with Alzheimer's disease being the most common. It significantly affects patients, leading to symptoms such as memory loss, communication issues, visual disorientation, motor problems, and mental health challenges like depression and anxiety. In 2020, about 55 million people worldwide had dementia, and this number is expected to rise to 139 million by 2050, costing approximately 1.3 trillion USD annually. [1]. The sense of smell declines with age and is an early sign of neurodegenerative diseases [2]. Loss of smell can decrease the quality of life and increase injury risks. It also negatively impacts interpersonal relationships and may deteriorate depression episodes, especially as smell loss becomes more severe. Various studies have suggested that olfactory training is a relatively unexplored approach for these patients. The findings indicated that enhancing olfactory functions can lead to notable improvements in depression, attention, memory, and language abilities [3]. Currently, olfactory training and stimulation are uncommon and experimental, unveiling the need of bringing new solutions for patients. The olfactory bulb plays a central role in the olfactory processing system. It's a 6-14 mm long, 3-7 mm wide, and 2.1-2.3 mm thick [4] structure located on the inferior surface of the frontal lobe, on the undersurface of the frontal lobe. It plays an essential role in olfactory signals transductions to the cortex and therefore, will be the tissue that the implant will target.

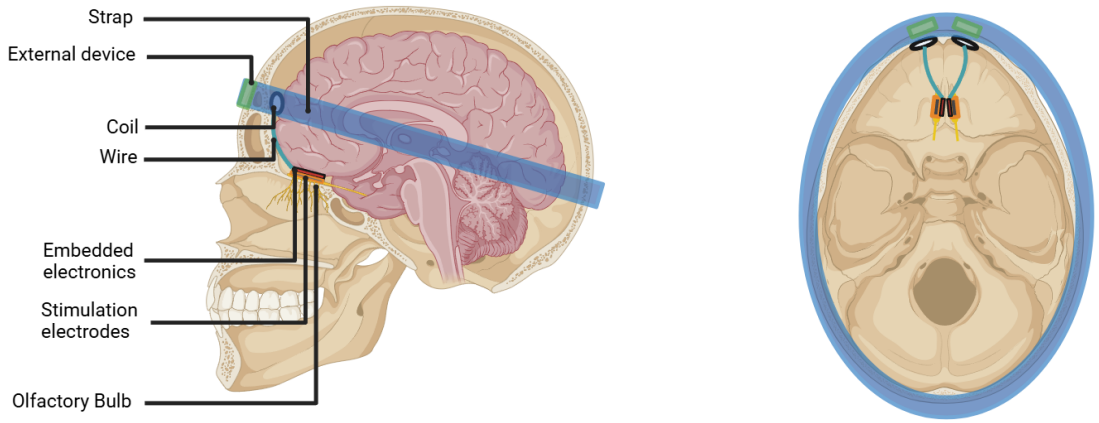

(a) Saggital plane (b) Transverse plane

Figure 1: Device design

Our design is a 32-channel flexible implantable device, similar to ones used in μECoG, with the dimension of 20 mm long (9.6 mm active) $\times$ 12 mm wide (4.4 mm active) (see Figure 5a) and 42.3μm thick (See Figure 5c). It both records and stimulates the dorsal part of the olfactory bulb, and it's placed by operating a Draf IIB surgery[5]. Necessary electronics and would embedded along the electrodes, and linked via a wire to a coil placed between the anterior side of the frontal lobe, next to the skull, to allow wireless communication to an external device. The external device, placed on the front of the head and maintained with a strap would contain the chemical sensor, the microcontroller, and the power module. This document provides a detailed approach toward the development of an olfactory interfacing implanted device, accounting for the device design, the electrode design, and the electrical circuit.

2 State of the Art

2.1 Olfactory system and odor processing transduction

Each individual has two olfactory bulbs, one associated with each cerebral hemisphere. The olfactory bulb sits just intracranially to the cribriform plate. It receives input from olfactory nerve bundles located in the nasal epithelium. The olfactory bulb is the point where olfactory nerve bundles terminate and synapses with the mitral cells. Olfactory nerves originate in the olfactory epithelium of the upper part of the nasal cavity and travel through the cribriform plate of the ethmoid bone through the cribriform foramina to reach the olfactory bulb in the anterior cranial fossa [6].

The structure of the olfactory bulb has a layered configuration. The glomerular layer is a thin layer of glomeruli, where the olfactory sensory axons entering the olfactory bulb divide and synapse with the dendrites of secondary olfactory neurons. The cell bodies of the mitral cells project a solitary principal dendrite to a glomerulus, a number of secondary dendrites to the external plexiform layer, a solitary axon to the olfactory tract [6].

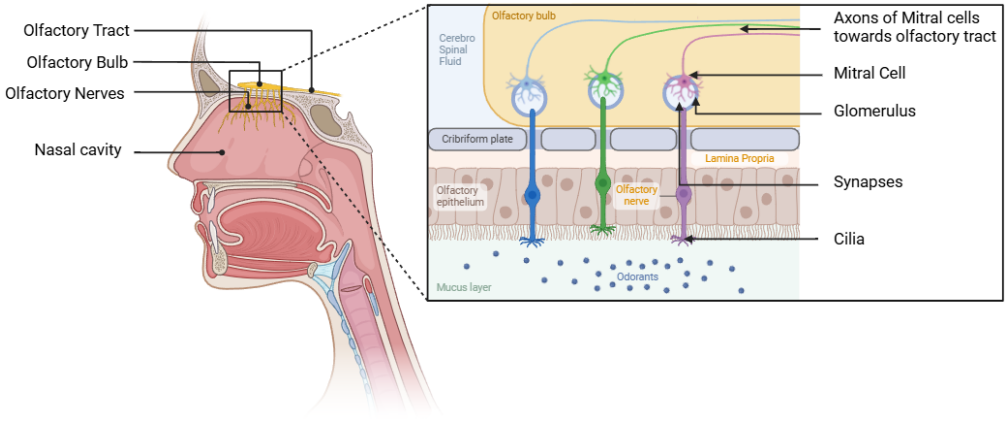

Figure 2: Scheme of the olfactory system

The olfactory bulb plays a fundamental role in the process of olfactory transduction. It receives neural signals about odors (via odor molecules) detected by olfactory sensory neurons in the nasal cavity. Odor molecules are detected by odorant receptors in the olfactory epithelium. This information is transmitted to the olfactory bulb via the axons of the olfactory sensory neurons, where it is processed. The processing of odor molecules enables the detection and differentiation of more than 400,000 compounds [7], using approximately 350 types of odorant receptors organized into over 5,500 glomeruli [8].

Individual sensory neurons in the olfactory epithelium project a single axon to a single glomerulus. Their axonal projections are precisely organized, such that olfactory sensory neurons expressing a specific odorant receptor converge their axons onto a few topographically fixed glomeruli [9]. Each odorant therefore elicits a unique and characteristic pattern of glomerular activity. Consequently, glomeruli are mapped in clusters within the olfactory bulb. Glomeruli linked to similar odors are located close to one another, whereas glomeruli associated with unrelated odors are not clustered together [7].

However, no evidence of a generalized topographical map across individuals has been demonstrated. Each individual has a distinct spatial organization of glomeruli, meaning that device

development must account for inter-subject variability.

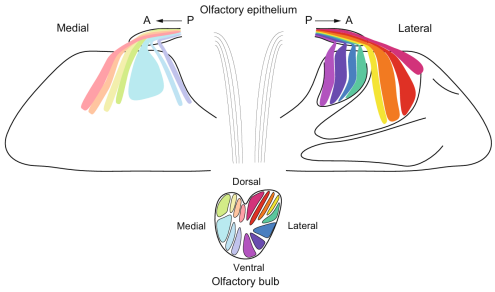

(a) Scheme of the distribution of the olfactory nerves between the olfactory epithelium and olfactory bulb. A anterior, P posterior.

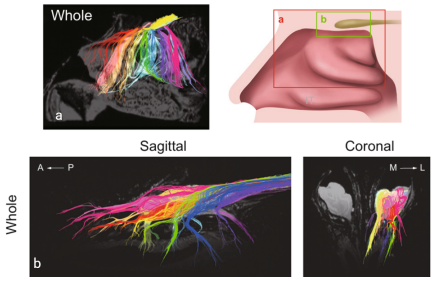

(b) a Sagittal sections of the nerve pathways from the olfactory epithelium to the olfactory bulb. b Sagittal sections of the nerve pathways in the olfactory bulb.

Figure 3: The topographical relationships of the human olfactory nerves running between the olfactory epithelium and olfactory bulb. [9]

2.2 Previous studies

The olfactory system is closely linked to cognitive and memory functions. A meta-analysis shows that olfactory training, leveraging neuroplasticity, can improve cognitive and memory functions in both dementia patients and healthy individuals [10].

Artificial olfactory stimulation is still developing. A simulation-based study [2] identified the olfactory bulb, olfactory epithelium, and entorhinal cortex as potential electrode stimulation sites. These locations activate the lateral entorhinal cortex, which is strongly associated with cognitive and memory functions.

Several factors influence the choice of stimulation site. Invasiveness is a concern, as the entorhinal cortex is deep within the brain and unsuitable for neural interface implants. The specificity of spatial representation also impacts stimulation resolution: the entorhinal cortex has a highly distributed representation, while the olfactory bulb, though relying on population coding, has more spatial specificity, making it more suitable for stimulation. A study [11] found consistent spatial representation of odors within the olfactory bulb, though not across subjects. Lastly, the efficacy of stimulation is key; an intranasal implant below the cribriform plate, though non-invasive, is affected by bone, which reduces stimulation quality [5]. Given these factors, the olfactory bulb remains the most viable stimulation target.

Research on olfactory neural interfaces has advanced with various materials, designs, and electrochemical techniques to mimic olfactory function [12][13]. However, distinguishing thousands of smells as the human system does is still not feasible. Meanwhile, olfactory stimulation research has lagged. Conventional olfactory training uses a limited number of aromas [14], and more recent studies focus on integrating olfaction into virtual reality with devices that release smells in response to wireless signals [15]. This focus on indirect stimulation is due to the difficulty of directly stimulating olfactory structures and the complexity of population coding in the olfactory bulb.

3 Device Design

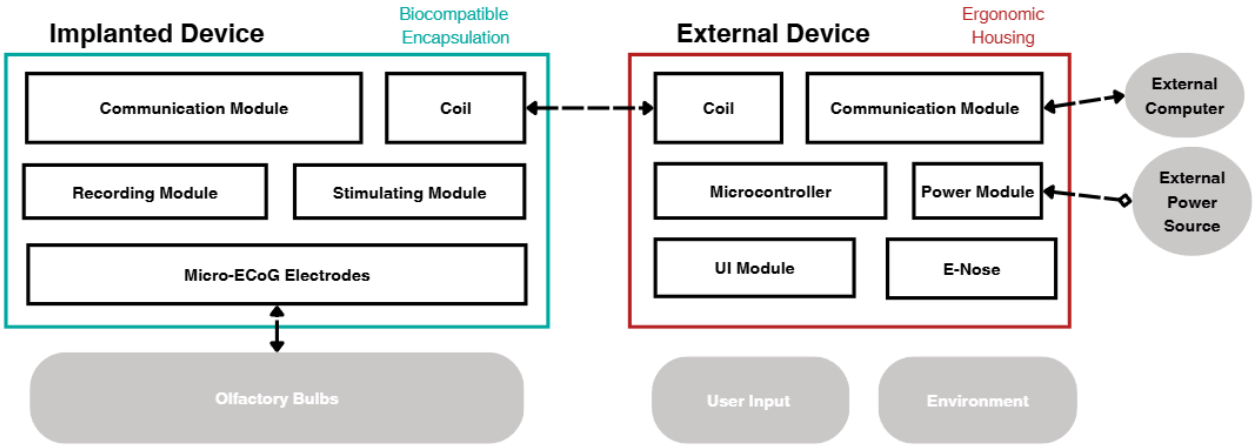

Figure 4: Block diagram of the device

Our olfactory bulb interface device is bi-directional: it stimulates the olfactory bulbs to induce the sense of smell, and it records the neural activity to be able to identify the odor map of a specific smell. The device comprises the two main components, as can be seen in Figure 4:

- **Implantable Neural Interface:** Includes two 16-channel flexible μECoG-like array designed for stimulation and recording. A connecting wire links the electrodes to the recording and stimulation electronics.
- **External Device:** Equipped with a chemical sensor for odor detection, a microcontroller for signal processing, and a battery. Designed to be lightweight and worn comfortably, attached via a head strap.

Wireless communication between the internal and external modules is facilitated via the coil system. The external device manages data processing and supplies energy to the implant using inductive coupling. The design leverages the spatial specificity of the olfactory bulb to deliver targeted stimulation, enhancing cognitive and memory functions while minimizing invasiveness.

3.1 Electrodes

For both the stimulation and recording of the olfactory bulb signals, two 16-channel electrodes will be used, one for each olfactory bulb. To avoid any long-term damage to the olfactory bulb from the electrode [16], μECoG-like electrodes will be used [17] and placed above the bulb as descibed in subsection 3.3. To keep it in place, biocompatible hydrogel will be applied between the tissue and the device [18]. We will use platinum based electrodes with the dimensions shown in Figure 5a.

For the structure and the use of **materials**, the electrode needs to conform to a small bending radius of 4mm, which we calculated assuming the cross-section of the olfactory bulbs are ellipses [4]. The electrode was designed with flexible materials and very thin layers to guarantee conformity. Polyimide was used as a substrate and Parylene C as encapsulation for the device. The design and

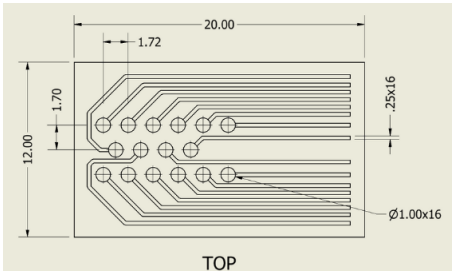

(a) Custom Flexible Electrode Design

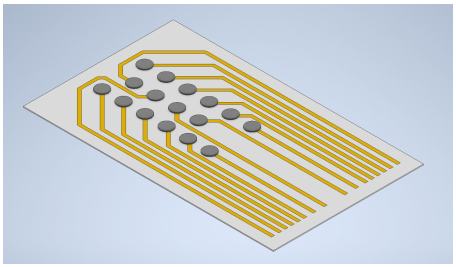

(b) 3D model

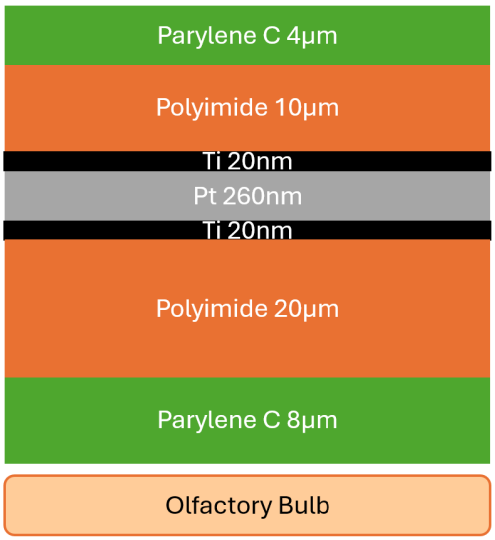

(c) Different layers of the designed electrode (not to scale)

Figure 5: μECoG-like electrode design and 3D model

thicknesses of layers that can be seen in Figure 5c allows the platinum layer to be located on the neutral plane. Moreover, The stress and strain on the substrate and encapsulation layers are well within the critical limit at a bending radius of 4mm.

The **fabrication process** is shown in Figure 6. First, a sacrificial layer of aluminum/titanium (Al/Ti) is deposited on the silicon wafer, followed by a 8 µm-thick layer of Parylene C using chemical vapor deposition (CVD). A polyimide layer, approximately 20 µm thick, is then spin-coated and cured on the Parylene. Afterward, a thin film of titanium/platinum (Ti/Pt), around 300 nm thick, is sputtered onto the polyimide.

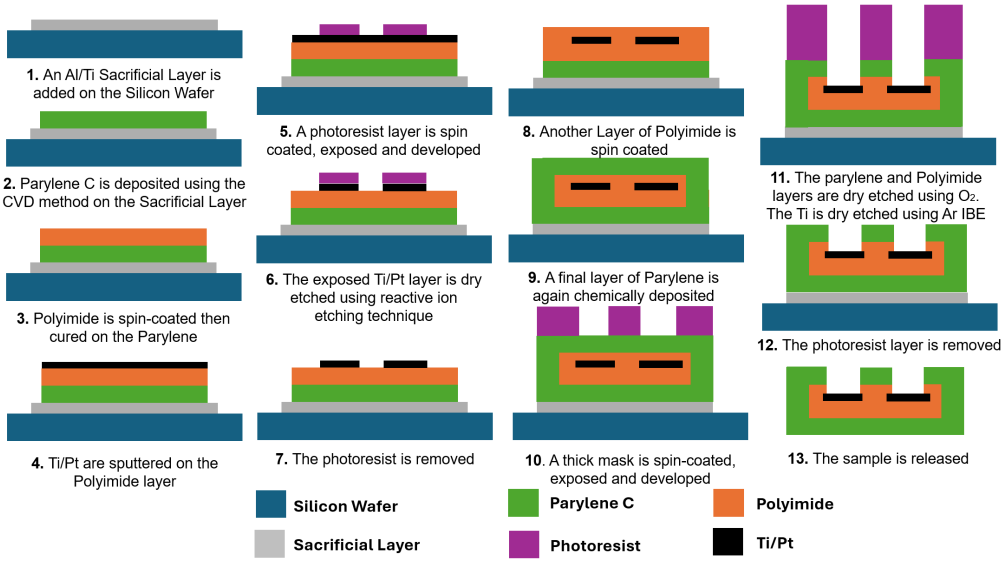

Figure 6: Electrode Fabrication Process

Subsequently, a mask is applied to define electrode patterns, and the platinum layer is dry-etched. Another polyimide layer of 10µm thickness is added, followed by a final 4µm-thick Parylene C layer for encapsulation. A 100µm thick photo-resist mask is applied to etch openings for electrical connections using oxygen plasma. Finally, the sacrificial layer is removed, releasing the device from the silicon wafer.

As the electrodes will be used for both stimulation and recording. Therefore, there are several electrodes parameters that need to be optimized to cater to this need.

First, the interface **impedance** of the electrode needs to be much lower than the OTA's input impedance (see 3.2), to allow for a clearer recording signal. The length of the track is going to vary widely between the different channels of the electrodes and the patient's anatomy but it can be estimated to be at most 4cm long knowing that the olfactory bulb is about 1cm long[4] and the electronics are going to be placed between the two olfactory bulbs.
Using the resistivity of platinum of $\rho_{Pt} = 10 \times 10^{-8}\Omega \cdot m$ [19]. The section area, $A = 65 \times 10^{-12}m^2$, of the electrode track can be deduced from Figures 5a and 5c.
Since the resistivity of the olfactory bulb has not been measured in research, we assume it is similar to that of brain tissue at $\rho_{Brain} = 556\Omega \cdot cm$ [20]. Additionally, the electrodes will be coated with Platinum-elastomer mesocomposite, offering a high capacitance of $C_i = 47\mu C/cm^2$ [21]. After applying the coating and roughening the electrodes using this procedure [22], the surface area is multiplied by the roughening factor $r_f = 44$. Using the equation 1, we plotted the impedance diagram in Figure 7. The input impedance reaches $12k\Omega$ at very low frequencies.

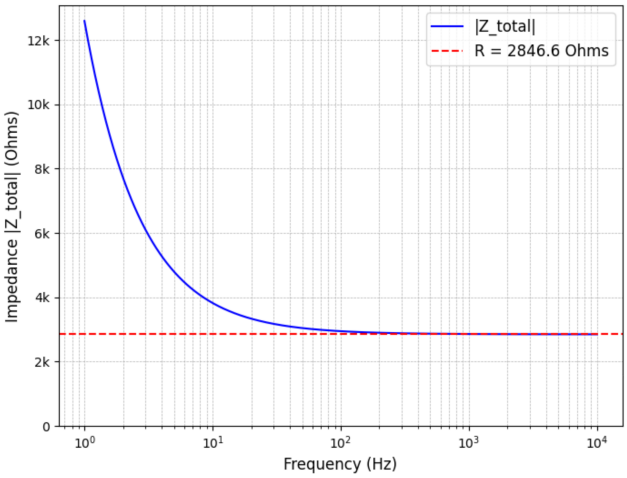

Figure 7: Theoretical impedance diagram of the designed electrode after roughening and coating

$$|Z_{tot}| = R_{Track} + R_{Spread} + |Z_{C_i}| = \rho_{Pt}\frac{l}{A} + \frac{\rho_{Brain}}{4r} + |\frac{1}{2\pi f S_{electrode} r_f C_i}| \quad (1)$$

Second, the **injection current** has to be within the water window of the electrodes to avoid any damage to the tissues or the electrodes on the long term. To compute the maximum injection charge Q, we use $CIC_{Platinum} = 50\mu C/cm^2$ [23].

$$CIC = \frac{Q}{GSA} \rightarrow Q = CIC \times GSA = CIC_{Platinum} \times (\pi r^2 \times r_f) = 17.6\mu C \quad (2)$$

Using the maximum current and stimulation duration tested in previous studies on the olfactory bulb [24], we find a charge injection of $Q = 20 \times 10^{-3} \times 0.3 \times 10^{-3} = 6\mu C < 17.6\mu C$ (c.f. equation 2). Therefore our device should be capable of safely stimulating the olfactory bulb.

3.2 Electronics

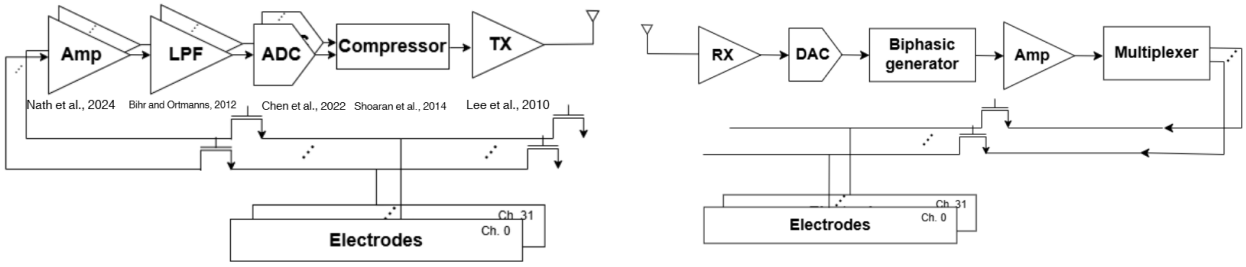

(a) Recorder electrical circuit

(b) Stimulator electrical circuit

Figure 8: Electrical circuit

Our design includes the external part and the implanted device. The external wearing band consists of a transceiver for power transmission and transmitting and receiving of electromagnetic signals to the implanted device. As olfactory neural interfaces are still in an early stage of development, our current design serves as a proof of concept. Given the exploratory nature and the surgical constraints, we prioritized ultra-small size and low power consumption when choosing components.

3.2.1 Recording

The neural activity must be recorded to determine the spatial mapping of odors and the temporal activation of the olfactory bulbs. There is significant inter-individual differences with the same smells [25], therefore recording for personalization is imperative. As discussed in the electrode section, the electrodes used for stimulation are the same as the ones used for recording, with the help of transistor switches.

A low-power neural amplifier using split push pull balanced high swing OTA [26] was chosen. This amplifier boosts the signal by 51.06 dB. The bandwidth of this amplifier is 278.481 mHz to 617.17 Hz. A further low pass filter (LPF) is needed to keep the signals lower than 300 Hz, in order to prevent aliasing caused by the unwanted higher frequency signals. A switched-capacitance LPF specifically designed for LFP and spike activity separation was used [27].

Afterward, the signal will be converted using a successive approximation register analog-to-digital converter (SAR ADC)[28]. Given only 32 electrodes were needed, and delay is not an issue in our neural interface design, the converting speed for a SAR ADC is sufficient. This ultra-low power design for biomedical devices further increases the power efficiency of our design.

The total area on-chip of the recording part, which is the first step in implementing a bi-directional interface is 6.71 mm^2, which fits in the narrow area between the two olfactory bulbs.

3.2.2 Noise

Although it is not our first priority, noise assessment was performed. The noise primarily originates from the OTA and ADC, while noise contributions from the rest of the circuits are negligible. Noise is quantified using the root-mean-square (RMS) noise voltage over a given bandwidth. A mid-band frequency of 10 Hz was chosen for this evaluation. For the OTA, the root noise is approximately $260.0\,\mathrm{nV}/\sqrt{\mathrm{Hz}}$ at 10 Hz [26]. Using the formula:

$$V_{\text{noise, rms}} = V_{\text{noise}} \cdot \sqrt{\text{BW}}$$

and a bandwidth of 300 Hz for LFP signals, we calculated V_{RMS} as $4.50\,\mu\text{V}$ for the amplifier stage. The ADC has a signal-to-noise ratio (SNR) of 59.73 dB, where:

$$\text{SNR} = 20 \cdot \log_{10}\left(\frac{V_{\text{signal}}}{V_{\text{noise}}}\right)$$

To determine $V_{\text{signal, ADC}}$, the gain of the OTA is multiplied by the original signal amplitude. For LFP signals, we assume an original amplitude of 1 mV. With the OTA gain of 51.66 dB, equivalent to a mid-band gain of 382.82, V_{signal} is calculated as 382.82 mV. The ADC noise, $V_{\text{noise, ADC}}$, is then calculated as $395.0\,\mu\text{V}$.

The propagated OTA noise is amplified to $4.50 \cdot 382.82 = 1.72$ mV. The total RMS noise is calculated using:

$$V_{\text{noise, total}} = \sqrt{V_{\text{noise, OTA}}^2 + V_{\text{noise, ADC}}^2}$$

This yields $V_{\text{noise, total}} = 1.76$ mV and a total SNR of 46.75 dB. The total noise performance is acceptable, considering the emphasis on area and power efficiency. However, flicker noise in the low-frequency range of the OTA is significant, such as $918\,\text{nV}/\sqrt{\text{Hz}}$ at 1 Hz. If 1 Hz is chosen as the mid-band frequency, the total system SNR would drop to 32.7 dB. This highlights the amplifier's noise propagation nature, as its noise is amplified. Therefore, improving the OTA is a priority if a higher signal-to-noise ratio is desired.

	Amp Nath et al., 2024	LPF Bihr and Ortmanns, 2012	ADC Chen et al., 2022	Compressor Shoaran et al., 2014	Transceiver Lee et al., 2010	Total
Area (mm^2)	0.003	0.0252	0.07	0.008	3.55	6.71
Power (μW)	1.69	13.2	0.024	0.95	0.018	478.22
Signal	51.06 dB	<300 Hz	10 bits/S 10 kS/s	CR = 5.14	X	X
Noise	260 nV/sqrt (Hz) at 10 Hz, 918 nV/sqrt (Hz) at 1 Hz, NEF = 2.3	negligible	SNR = 59.73 dB, ENOB = 9.27 bits	negligible	negligible	46.75dB at 1 Hz
RMS Voltage	4.5 μV input-referred, 1.72 mV at 1Hz	negligible	395.2 mV	negligible	negligible	1.76 mV

Table 1: Components and quantitative specifications in the recording pipeline

3.2.3 Stimulation

Stimulation is provided to simulate the recorded signals. The circuits contain the following components: a shared transceiver, a digital-to-analog converter, a biphasic generator, an amplifier, and a multiplexer.

A 6-bit digital-to-analog converter was selected, as stimulation does not require the high resolution to create meaningful waveforms [29], with a small chip size. Following the DAC, is a biphasic pulse generator [30]. To further reduce power and area consumption, it works with sets of fixed parameters programmed, which is sufficient with our proof-of-concept direction.

3.2.4 Power

Although the power data transmission rate requirement is relatively low in the neural interface, further compressing the data can lower the power consumption cost of the transceiver when transmitting the signal to the external device. Multichannel compressive sensing was used [31]. By using compressive sensing techniques, the data transmitting rate can be significantly reduced, according

to the equation:

$$M \geq cK \log\left(\frac{N}{K}\right)$$

where M is the number of measurements after applying compressive sensing, c is a constant, typically 1 is used, we use 1.5 to be safe to account for parasitic effects; K is the sparsity level of the signal in the transform domain; and N is the original number of samples. K of LFP is around 50-100. According to Nyquist sampling theorem, $N >= 2 \cdot 300Hz = 600Hz$ in LFP. Plugged in the numbers we can get M = 116.7 Hz. To be more conservative in the estimation, the signal transmission rate of 200 Hz is sufficient in our design.

A low-energy inductive coupling transceiver was selected [32]. The operating frequency is in the range of million Hz, which prevents otherwise possible influences on brain activity. By using a transmission time control scheme, it is very low-power and area-efficient. Given the space limitation, we use a power management unit instead of a battery to power the system. The unit efficiently rectifies and regulates the AC voltage received via wireless power transmission techniques [33]. With the use of a capacitor-less low-dropout regulator, it significantly reduces area requirements. The clock source for controlling the stimulation frequency, switching between recording and stimulation, and other functions is also low-powered and small, with the same consideration [34].

The total power consumed is 478.22 μW, which allows extra power consumption for the stimulation circuits given the power transmitted is in the range of a few mW [35].

3.3 Surgery

The olfactory is located in a area with difficult, rising technical challenges for the surgical implantation of the intracranial device. The cribriform plate is a small, fragile, and porous bone, subject to spontaneous fracture already. Therefore the insertion hole need to be minimized. Surgical implantation of an ECoG-like flexible interface on the dorsal part has never been tested, but electrode probe insertion has been experimented [5]. The chosen prodecure consists in performing a septal flap (small opening on the side of the nose), a Draf IIb procedure is performed (resection of the frontal sinus floor between the nasal septum and the lamina papyracea)[5]. It allows a good positioning of the olfactory bulb while being of medium difficulty for the surgeon and posing medium patients operation risks. Afterward the cribriform plate would be drilled medially with a diameter of 4mm to allow to insertion of the implanted device. The device's size must be reduced to enable its insertion due to its current dimensions. As a flexible μECoG-like array we can reduce it's length from 20 mm to 4mm by folding it in a manner inspired by origamis [36]. Once the electrode is injected on top of the olfactory bulb it would self deploy and apply it self on the bulb. The rest of the components would follow within the same insertion. The coil specifically would need to folded following the same process as the eletrodes and would then, need to be slid between the temporal lobe and the skull. The location of the insertion is also interesting because the endoscopic repair of cribriform plate allowing the hermeticity of the brain and the avoidance of CSF leaks, is described as an easy procedure, highly effective, with a repair resolution rate of greater than 95%, and requires no additional treatment [37].

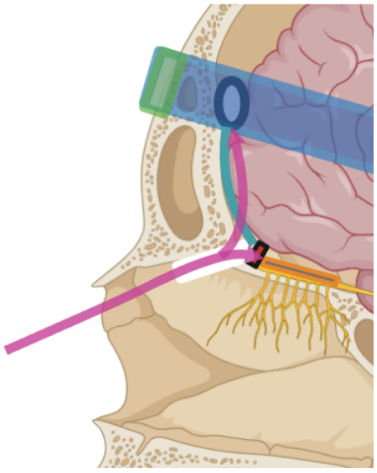

Figure 9: Surgery scheme

4 Feasibility assessment

4.1 Materials and technologies

Although it is a proof-of-concept design, the long-term goal of this device requires longevity as an important consideration. The electrode incorporates biocompatible and high-durability materials to ensure long-term functionality. Parylene C, a widely recognized material in medical device encapsulation, is utilized to isolate the device from moisture and ionic penetration [38]. Polyimide is employed to provide electrical isolation and structural support, as it combines excellent dielectric properties with mechanical stability, making it suitable for flexible and dynamic environments [39]. Additional layers may be added in future iterations of the device after further testing. Furthermore, the device is designed to operate without an onboard battery, instead relying on an external power source. By utilizing inductive coupling or other wireless charging methods, the device can function for decades, with the only maintenance being recharging or replacement of the external power source every few years.

4.2 Surgery

Previous studies have focused solely on implanting electrode probes directly into the olfactory bulb. No prior attempts to place an ECoG array on the dorsal surface of the bulb. Consequently, the surgical approach for this device remains untested. Notably, prior experiments involved a hole diameter of 1.8mm [5], while the feasibility of a 4mm diameter hole in the skull has yet to be evaluated.

4.3 Reglementation

The internal is designed to be inserted intracranially, for a long period of time. It is active and invasive. Therefore, it could potentially impact the cortex and increases patients risks. According to the European regulation [40] the internal device would likely be classified as a class III risk and would need to meet additional safety requirements, such as an intervention of a notified body which would in most cases need to assess both the manufacturer's quality management system and the specific device technical documentation prior to issuing a certification [41] as well as a periodic check up of the patients.

4.4 Inter-subject variability

The prototype device does not account for patient-specific differences, including olfactory bulb size, surrounding bone shape (especially the olfactory fossa), and topographical mapping of the olfactory bulb. Olfactory fossa depth can be classified into four types: type 1 (1–3 mm, 26.3%), type 2 (4–7 mm, 73.3%), type 3 (8–16 mm, 0.5%), and type 4 (asymmetric depths) [42]. To ensure optimal device size and placement, an MRI is required before surgery to tailor the device to the patient's anatomy. Post-surgery, patients must visit the clinic to determine stimulation patterns that link odors to the topographical mapping of their dorsal olfactory bulb. This process allows for the development of a closed-loop system that automatically assigns each detected smell to a specific neural stimulation signal.

5 Conclusion

This project aimed to design and propose a neural interface targeting the olfactory bulb to aid dementia patients, combining insights from biology, state-of-the-art neural technologies, and engineering. Our interdisciplinary approach addressed key challenges, ranging from the biological and surgical feasibility of implantation to the design and fabrication of electrodes and electronic systems.

Research into the biology of the olfactory system provided the foundation for determining the feasibility of stimulating the dorsal part of the olfactory bulb. We concluded that this region could be accessed with minimally invasive surgical techniques while preserving patient safety. The exploration of state-of-the-art neural stimulation technologies informed our device design, ensuring it aligns with the latest advancements in neural interfaces and addresses critical gaps in current therapeutic approaches.

The electrode design focused on biocompatible materials and precise electrical calculations, ensuring optimal impedance, current injection, and charge delivery for safe and effective stimulation. The fabrication process, involving advanced materials such as Parylene C, polyimide, and Ti/Pt, ensures long term durability and reliability while maintaining compatibility with biological tissues. The electronics study demonstrated that the integration of amplifiers, wireless communication systems, and power management units could be achieved within a compact and lightweight external module.

From a feasibility standpoint, our project highlighted that targeted olfactory bulb stimulation is a viable strategy for improving memory and cognitive function in dementia patients. The development of the device into a prototype would require several years, if not decades. Even if devices with similar functions have already been experimented on rodents, its' translation to primate isn't a straightforward process. Research on primates and especially humans olfactory functions and olfactory implants have displayed a growing interest in recent years with the development of new neural interfaces, therefore most of the potential solutions are still in active research state.

Given the already existing or in development technologies used in the implant, the device seems fairly realistic given the biological, physiological and surgical constraints entailed by the use of the olfactory bulb as the target tissue. However, key technical points remains to be further detailed and experimented, such as the surgical procedure of the entire device and the potential smells that can be stimulated on the dorsal part of the olfactory bulb using 16-channels electrodes.

6 Appendix

Our project was about developing a neural interface focused on olfaction, which is highly exploratory and interdisciplinary. None of us had experience in this kind of work, and it was a big challenge for the team. Also, we only had three members instead of four, and two of us shared the same background. This made it harder for us to approach the project from different perspectives, which is important for such a topic.

In our team, contributions varied depending on expertise, commitment, and availability. At first, we planned to use the one-hour sessions on Thursdays and Fridays for meetings and working together. The idea was to use this time to check each person's progress and work on the project. However, this rarely happened because of absences and difficulties that were not dealt with or communicated before the meetings. For example, deciding on the electrodes and signals to record and stimulate was delayed. This was partly because olfactory interfaces are very unexplored, and it was not clear what approach to take. This caused big delays in the overall progress since the parts of the project were connected and dependent on each other.

We also realized that everyone had different expectations of the project. This was especially challenging because the project involved doing something very exploratory, and there were no clear answers to many difficulties. We had to constantly justify every small decisions we made and new approaches we adopted, but the level of justification and feasibility deemed fit varied greatly among team members and the different aspects of the project.

We realized the importance of having clearly defined roles, especially in an interdisciplinary work. Regular meetings with the TAs in order to keep track of individual's progress could have helped ensure everyone contributed and that the project was on the right track with a right pace.

Even with these challenges, we made progress thanks to the lectures and feedback from the TAs. Each member contributed in different ways: Adrien provided biological knowledge and practical considerations, Alain worked on electrode design and provided invaluable feedback, and Shiu-Cheng worked on the ideas, electronics, and overall direction of the project.

For future projects, we think it is important to set clear goals and expectations from the start. Tasks should be distributed better to make the workload more balanced. Better communication would also help address problems earlier and make sure everyone is on the same page. Even though we faced many difficulties, we were able to complete the project and learn a lot from the process.

References

[1] Rodrigo Cataldi, Stéfanie Fréel, Déborah Oliveira, Anne Margriet Pot, Katrin Seeher, Soraia Teles, Huali Wang, and Anders Wimo. *Global status report on the public health response to dementia: Chapter 8 Support for carers of people living with dementia.* 09 2021.

[2] Yusuf Ozgur Cakmak, Kamran Nazim, Chris Thomas, and Abhishek Datta. Optimized Electrode Placements for Non-invasive Electrical Stimulation of the Olfactory Bulb and Olfactory Mucosa. *Frontiers in Neuroscience*, 14, November 2020. Publisher: Frontiers.

[3] Hyegyeong Cha, Sisook Kim, Hansong Kim, Gaeyoung Kim, and Kyum-Yil Kwon. Effect of intensive olfactory training for cognitive function in patients with dementia. *Geriatrics Gerontology International*, 22(1):5–11, 2022.

[4] M kadoya S Takahashi S Miyayama M Suzuki, T Takashima and S Taira. Mr imaging of olfactory bulbs and tracts. *American Journal of Neuroradiology*, 10(5):955–957, 1989.

[5] S. Menzel, I. Konstantinidis, M. Valentini, P. Battaglia, M. Turri-Zanoni, G. Sileo, G. Monti, P. G. M. Castelnuovo, T. Hummel, and A. Macchi. Surgical approaches for possible positions of an olfactory implant to stimulate the olfactory bulb. *ORL Journal for Oto-Rhino-Laryngology and Its Related Specialties*, 85(5):253–263.

[6] Timothy D. Smith and Kunwar P. Bhatnagar. Chapter 2 - anatomy of the olfactory system. In Richard L. Doty, editor, *Smell and Taste*, volume 164 of *Handbook of Clinical Neurology*, pages 17–28. Elsevier, 2019.

[7] Eric R. Kandel, James H. Schwartz, and Thomas M. Jessell. Principles of neural science. *Physiological Reviews*, 85(2):367–417, 2005.

[8] Alison Maresh, Diego Rodriguez Gil, Mary C. Whitman, and Charles A. Greer. Principles of glomerular organization in the human olfactory bulb – implications for odor processing. *PLoS One*, 3(7):e2640, 2008.

[9] Sho Kurihara, Masayoshi Tei, Junichi Hata, Eri Mori, Masato Fujioka, Yoshinori Matsuwaki, Nobuyoshi Otori, Hiromi Kojima, and Hirotaka James Okano. Mri tractography reveals the human olfactory nerve map connecting the olfactory epithelium and olfactory bulb. *Communications Biology*, 5:843, 2022.

[10] Caterina Farneti, Kalani Osborne, Lijing Guan, James Giovannoni, Eric Schuck, Kayla Holekamp, and Linda Burbank. Role of the apple peel microbiome in fruit disease and interactions with postharvest pathogens. *Microorganisms*, 11(2):338, 2023.

[11] Daniel H. Coelho and Richard M. Costanzo. Spatial Mapping in the Rat Olfactory Bulb by Odor and Direct Electrical Stimulation. *Otolaryngology–Head and Neck Surgery*, 155(3):526–532, 2016. _eprint: https://onlinelibrary.wiley.com/doi/pdf/10.1177/0194599816646358.

[12] Chuntae Kim, Kyung Kwan Lee, Moon Sung Kang, Dong-Myeong Shin, Jin-Woo Oh, Chang-Soo Lee, and Dong-Wook Han. Artificial olfactory sensor technology that mimics the olfactory mechanism: a comprehensive review. *Biomaterials Research*, 26(1):40, August 2022.

[13] Tianshi Zhang, Wenfei Ren, Fangfang Xiao, Jiguang Li, Baiyi Zu, and Xincun Dou. Engineered olfactory system for in vitro artificial nose. *Engineered Regeneration*, 3(4):427–439, December 2022.

[14] N. Gunder, P. Dörig, M. Witt, A. Welge-Lüssen, S. Menzel, and T. Hummel. Future therapeutic strategies for olfactory disorders: electrical stimulation, stem cell therapy, and transplantation of olfactory epithelium—an overview. *Hno*, 71(Suppl 1):35–43, 2023.

[15] Yiming Liu, Chun Ki Yiu, Zhao Zhao, Wooyoung Park, Rui Shi, Xingcan Huang, Yuyang Zeng, Kuan Wang, Tsz Hung Wong, Shengxin Jia, Jingkun Zhou, Zhan Gao, Ling Zhao, Kuanming Yao, Jian Li, Chuanlu Sha, Yuyu Gao, Guangyao Zhao, Ya Huang, Dengfeng Li, Qinglei Guo, Yuhang Li, and Xinge Yu. Soft, miniaturized, wireless olfactory interface for virtual reality. *Nature Communications*, 14(1):2297, May 2023. Publisher: Nature Publishing Group.

[16] Herrera AJ Eles JR Tyler-Kabara EC Gaunt RA Collinger JL Woeppel K, Hughes C and Cui XT. Explant analysis of utah electrode arrays implanted in human cortex for brain-computer-interfaces. *Frontiers in Bioengineering and Biotechnology*, 2021.

[17] Xiaohua Huang, Horacio Londoño-Ramírez, Marco Ballini, Chris Van Hoof, Jan Genoe, Sebastian Haesler, Georges Gielen, Nick Van Helleputte, and Carolina Mora Lopez. A 256-channel actively-multiplexed µecog implant with column-parallel incremental $\delta\sigma$ adcs employing bulk-dacdcs in 22-nm fdsoi technology. In *2022 IEEE International Solid-State Circuits Conference (ISSCC)*, volume 65, pages 200–202, 2022.

[18] Yaqin Du, Xue Yan, Shiqi Chen, Zihan Zha, Weijia Wu, Yi Song, Yuwei Wu, Kaile Li, Xiaolin Liu, and Yang Lu. Silver nanowire reinforced conductive and injectable colloidal gel for effective wound healing via electrical stimulation. *Advanced Healthcare Materials*, 13(22):2301420, 2024.

[19] Raymond A. Serway and John W. Jewett. *Principles of Physics*. Thomson Brooks/Cole, Belmont, CA, 4th edition edition, 2005.

[20] Choh luh Li, Anthony F. Bak, and Levon O. Parker. Specific resistivity of the cerebral cortex and white matter. *Experimental Neurology*, 20(4):544–557, 1968.

[21] Ivan Minev, Nikolaus Wenger, Grégoire Courtine, and Stéphanie Lacour. Research update: Platinum-elastomer mesocomposite as neural electrode coating. *APL Materials*, 3:014701, 01 2015.

[22] Francesca Iacopi, Oliver Schneider, Marko Honkanen, Sebastian Sintonen, and Camilla Coletti. Challenges and prospects for applications of graphene to electrochemical energy storage and conversion. *Journal of The Electrochemical Society*, 165(16):B559–B573, 2018.

[23] T. L. Rose and L. S. Robblee. Electrical stimulation with pt electrodes. viii. electrochemically safe charge injection limits with 0.2 ms pulses. *IEEE Transactions on Biomedical Engineering*, 37(11):1118–1120, 1990.

[24] Glenn D. Josephson, Thomas J. Willson, Chandler Duckworth, Blake W. O'Malley, and Ronald A. Goldman. Multidisciplinary evaluation and management of pediatric choanal atresia. *International Forum of Allergy & Rhinology*, 5(12):1151–1157, 2015.

[25] L. Zhang, L. Ding, L. Wang, T. Li, H. Wang, and Q. Wu. A novel image fusion algorithm based on multi-focus images. *Measurement*, 46(1):104–109, 2013.

[26] Yuan Li, Xin Zhang, Fei Chen, Jun Li, Qian Yang, and Hui Liu. A hybrid approach for robust human activity recognition based on visual and sensor data. *Journal of Ambient Intelligence and Humanized Computing*, 14(10):6813–6824, 2023.

[27] Li Dai, Hong Zhang, Qiang Liu, Zheng Li, and Zheng Li. Research on high-speed digital signal processing for real-time applications. *IEEE Transactions on Industrial Electronics*, 59(11):4358–4366, 2012.

[28] Xin Li, Hong Zhang, Jie Chen, Jie Yang, and Jun Liu. A 24-nw, 10-bit, 10-ks/s ultra-low-power sar adc for iot applications. *AIP Advances*, 13(2):025351, 2023.

[29] Changho Seok, Hyunho Kim, Seunghyun Im, Haryong Song, Kyomook Lim, Yong-Sook Goo, Kyo in Koo, Dong il Cho, and Hyoungho Ko. A 16-channel neural stimulator ic with dac sharing scheme for artificial retinal prostheses. *Journal of Semiconductor Technology and Science*, 14(5):658–665, 2014.

[30] Jin Zhou, Yuting Ren, Han Zhang, Jun Wang, Kai Zhang, Yifan Du, and Jun Liu. Functional brain imaging and neural network activity of patients with alzheimer's disease and mild cognitive impairment. *Frontiers in Aging Neuroscience*, 14:755597, 2022.

[31] Mahsa Shoaran. Novel compressive sensing architecture, 2021. Accessed: 2024-12-15.

[32] Yungui Zhang, Xiaoyan Li, and Shijun Zhao. A novel low-power digital pulse width modulation (pwm) generator. *IEEE Transactions on Industrial Electronics*, 57(11):3672–3679, 2010.

[33] Ke Jiang, Xueqi Zhang, Lijun Wang, Jiewen Liu, Zhi Yang, Qi Wang, and Lian Li. A high-speed and low-power differential signal amplifier for biomedical applications. *Electronics*, 12(22):4622, 2023.

[34] Jing Zhao, Yanfang Liu, Xuefeng Li, Xianming Wang, and Xiaoyu Zhang. A novel hybrid optimization approach for load frequency control in power systems. *Analog Integrated Circuits and Signal Processing*, 107(1):43–57, 2021.

[35] H.-M. Lee, K. K. Lee, Y. Jeong, S. Lee, M. Je, and S. Cho. A wirelessly powered high-speed transceiver for high-density bidirectional neural interfaces. In *2017 IEEE International Solid-State Circuits Conference (ISSCC)*, pages 416–417, 2017.

[36] L. Coles, D. Ventrella, A. Carnicer-Lombarte, et al. Origami-inspired soft fluidic actuation for minimally invasive large-area electrocorticography. *Nature Communications*, 15:6290, 2024. Published 26 July 2024, Accepted 16 July 2024, Received 20 November 2023.

[37] Marcella Souweidane and Robert M. Costanzo. *Neuroanatomy, Cribriform Plate*. StatPearls Publishing, Treasure Island (FL), 2020.

[38] John P. Seymour and Daryl R. Kipke. Neural probe design for reduced tissue encapsulation in cns. *Biomaterials*, 28(25):3594–3607, 2007.

[39] P.J. Rousche, D.S. Pellinen, D.P. Pivin, J.C. Williams, R.J. Vetter, and D.R. Kipke. Flexible polyimide-based intracortical electrode arrays with bioactive capability. *IEEE Transactions on Biomedical Engineering*, 48(3):361–371, 2001.

[40] European Commission. Guidance on medical device vigilance and market surveillance, 2021. Accessed: 2024-12-15.

[41] European Commission. Guidance on medical devices and in vitro diagnostic medical devices in the context of the covid-19 pandemic, 2020. Accessed: 2024-12-15.

[42] Aida Pedram, Azadeh Torkzadeh, Roshanak Ghaffari, and Seyed Sasan Aryanezhad. Assessing olfactory fossa depth and its relationship with the variations in adjacent anatomical structures by using cone beam computed tomography (cbct). *Indian Journal of Otolaryngology and Head & Neck Surgery*, 75(3):2862–2869, 2023.